We are IntechOpen,
the world's leading publisher of
Open Access books
Built by scientists, for scientists

6,900
Open access books available

186,000
International authors and editors

200M
Downloads

Our authors are among the

154
Countries delivered to

TOP 1%
most cited scientists

12.2%
Contributors from top 500 universities

WEB OF SCIENCE™

Selection of our books indexed in the Book Citation Index
in Web of Science™ Core Collection (BKCI)

Interested in publishing with us?
Contact book.department@intechopen.com

Numbers displayed above are based on latest data collected.
For more information visit www.intechopen.com

8

Hydrodynamics Influence on Particles Formation Using SAS Process

A. Montes, A. Tenorio, M. D. Gordillo,
C. Pereyra and E. J. Martinez de la Ossa
Department of Chemical Engineering and Food Technology,
Faculty of Science, UCA
Spain

1. Introduction

Particle size and particle size distribution play an important role in many fields such cosmetic, food, textile, explosives, sensor, catalysis and pharmaceutics among others. Many properties of industrial powdered products can be adjusted by changing the particle size and particle size distribution of the powder. The conventional methods to produce microparticles have several drawbacks: wide size distribution, high thermal and mechanical stress, environmental pollution, large quantities of residual organic solvent and multistage processes are some of them.

The application of supercritical fluids (SCF) as an alternative to the conventional precipitation processes has been an active field of research and innovation during the past two decades (Jung & Perrut, 2001; Martín& Cocero, 2008; Shariati &Peters, 2003).Through its impact on health care and prevention of diseases, the design of pharmaceutical preparations in nanoparticulate form has emerged as a new strategy for drug delivery. In this way, the technology of supercritical fluids allows developing micronized drugs and polymer-drug composites for controlled release applications; this also meets the pharmaceutical requirements for the absence of residual solvent, correct technological and biopharmaceutical properties and high quality (Benedetti et al., 1997; Elvassore et al., 2001; Falk& Randolph, 1998; Moneghini et al., 2001; Reverchon& Della Porta, 1999; Reverchon, 2002; Subramaniam et al., 1997; Yeo et al., 1993; Winters et al.,1996), as well as giving enhanced therapeutic action compared with traditional formulations (Giunchedi et al., 1998; Okada& Toguchi, 1995).

The revised literature demonstrates that there are two principal ways of micronizing and encapsulating drugs with polymers: using supercritical fluid as solvent, the RESS technique (Rapid Expansion of Supercritical Solutions); or using it as antisolvent, the SAS technique (Supercritical AntiSolvent); the choice of one or other depends on the high or low solubility, respectively, of the polymer and drug in the supercritical fluid.

Although the experimental parameters influences on the powder characteristic as particle size and morphologies is now qualitatively well known, the prediction of the powder characteristics is not feasible yet. This fact it is due to different physical phenomena involved in the SAS process. In most cases, the knowledge of the fluid phase equilibrium is

necessary but not sufficient since for similar thermodynamic conditions, different hydrodynamics conditions can lead to different powder characteristics (Carretier et al., 2003).

So, the technical viability of the SAS process requires knowledge of the phase equilibrium existing into the system; the hydrodynamics: the disintegration regimes of the jet; the kinetics of the mass transfer between the dispersed and the continuous phase; and the mechanisms and kinetics of nucleation and crystal growth.

From the point of view of thermodynamics, the SAS process must satisfy the requirements outlined below. The solute must be soluble in an organic solvent but insoluble in the SCF. The solvent must also be completely miscible with the SCF, or two fluid phases would form and the solute would remain dissolved or partly dissolved in the liquid-rich phase. Thus, the SAS process exploits both the high power of supercritical fluids to dissolve organic solvents and the low solubility of pharmaceutical compounds in supercritical fluids to cause the precipitation of these materials once they are dissolved in an organic solvent, and thus spherical microparticles can be obtained.

On the other hand, characterization of hydrodynamics is relevant because of it is an important step for the success or the failure of the entire process, but with only some exception (Dukhin et al., 2005; Lora et al., 2000; Martín& Cocero, 2004), in the models developed for the SAS process, the hydrodynamics step received only limited consideration. For these reasons, the present review is focused on the investigation of the disintegration regime of the liquid jet into the supercritical (SC) CO_2. There are many works where correlations between the morphologies of the particles obtained in the drug precipitation assays and the estimated regimes were established (Carretier et al., 2003; Reverchon et al., 2010; Reverchon& De Marco, 2011; Tenorio et al., 2009). It was demonstrated that there are limiting hydrodynamic conditions that must be overcome to achieve a dispersion of the liquid solution in the dense medium; this dispersion must be sufficiently fine and homogeneous to direct the process toward the formation of uniform spherical nanoparticles and to the achievement of higher yields (Tenorio et al., 2009).

In this way, Reverchon et al. (Reverchon et al., 2010, Reverchon& De Marco, 2011) tried to find a correlation between particle morphology and the observed jet, concluding that expanded microparticles were obtained working at subcritical conditions; whereas spherical microparticles were obtained operating at supercritical conditions up to the pressure where the transition between multi- and single-phase mixing was observed. Nanoparticles were obtained operating far above the mixture critical pressure. However, the observed particle morphologies have been explained considering the interplay among high-pressure phase equilibria, fluid dynamics and mass transfer during the precipitation process, because in some cases the hydrodynamics alone is not able to explain the obtained morphologies, demonstrating the complexity of SAS processes. Moreover, the kinetics of nucleation and growth must also be considered.

2. Supercritical fluids

A supercritical fluid can be defined as a substance above its critical temperature and pressure. At this condition the fluid has unique properties, where it does not condense or evaporate to form a liquid or gas. A typical pressure-temperature phase diagram is shown in Figure 1. Properties of SCFs (solvent power and selectivity) can also be adjusted continuously by altering the experimental conditions (temperature and pressure). Moreover,
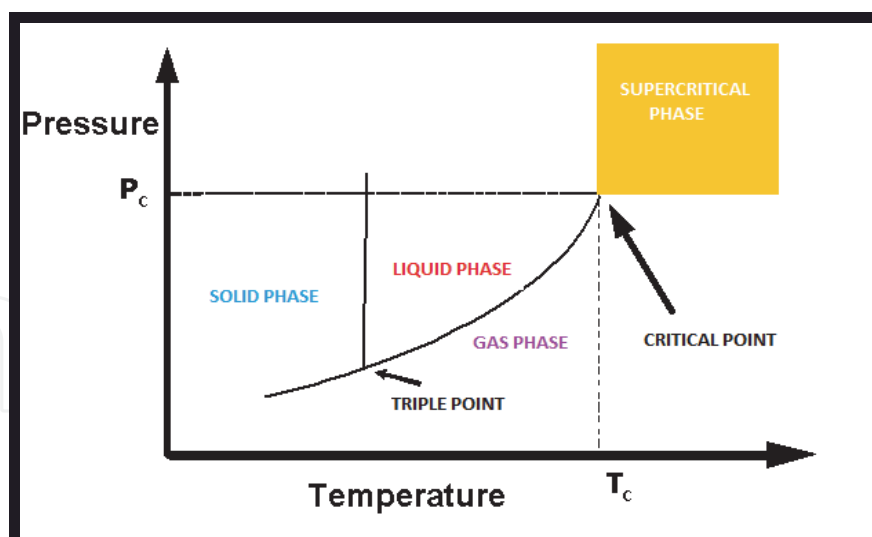
Fig. 1. Pressure-temperature phase diagram

these supercritical fluids have diffusivities that are two orders of magnitude larger than those of typical liquids, resulting in higher mass-transfer rates. Supercritical fluids show many exceptional characteristics, such as singularities in compressibility and viscosity, diminishing the differences between the vapor and liquid phases, and so on. Although a number of substances are useful as supercritical fluids, carbon dioxide has been the most widely used. Supercritical CO_2 avoids water discharge; it is low in cost, non-toxic and non-flammable. It has low critical parameters (304 K, 73.8 bar) and the carbon dioxide can also be recycled (Özcan et al., 1998).

3. Precipitation with SCF

The supercritical fluid technology has emerged as an important alternative to traditional processes of generation of micro and nanoparticles, offering opportunities and advantages such as higher product quality in terms of purity, more uniform dimensional characteristics, a variety of compounds to process and a substantial improvement on environmental considerations, among others.

Previously, it was discussed that the different particle formation processes using SCF are classified depending on how the SCF behaves, i.e., the supercritical CO_2 can play the role as antisolvent (AntiSolvent Supercritical process, SAS) or solvent (RESS process).

In the facilities of University of Cádiz, amoxicillin and ampicillin micronization have been carried out by SAS process (Montes et al., 2010, 2011a; Tenorio et al., 2007a, 2007b, 2008). Several experiments designs to evaluate the operating conditions influences on the particle size (PS) and particle size distribution (PSD) have been made. Pressures till 275 bar and temperatures till 338K have been used and antibiotic particle sizes have been reduced from 5-60 µm (raw material) to 200-500 nm (precipitated particles) (Figure 2).

The concentration was the factor that had the greatest influence on the PS and PSD. An increase in the initial concentration of the solution led to larger particles sizes with a wider distribution. Moreover, ethyl cellulose and amoxicillin co-precipitation has been carried out by SAS process (Montes et al., 2011b). SEM images of these microparticles are shown in Figure 3. It was noted that increasing temperature particle sizes were increased. Anyway, SEM images are not accurate enough to observe the distribution of both compounds
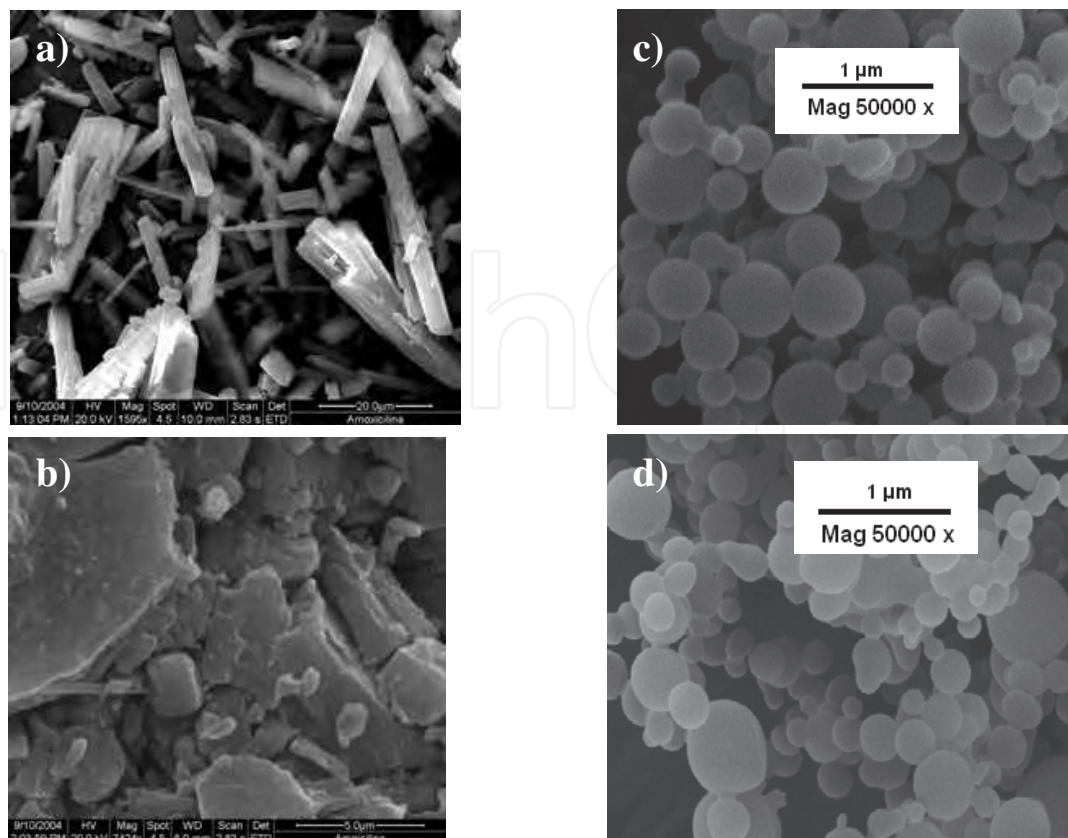
Fig. 2. SEM images of commercial a) amoxicillin and b) ampicillin, c) precipitated amoxicillin (Montes et al., 2010) and d) precipitated ampicillin (Montes et al., 2011a)
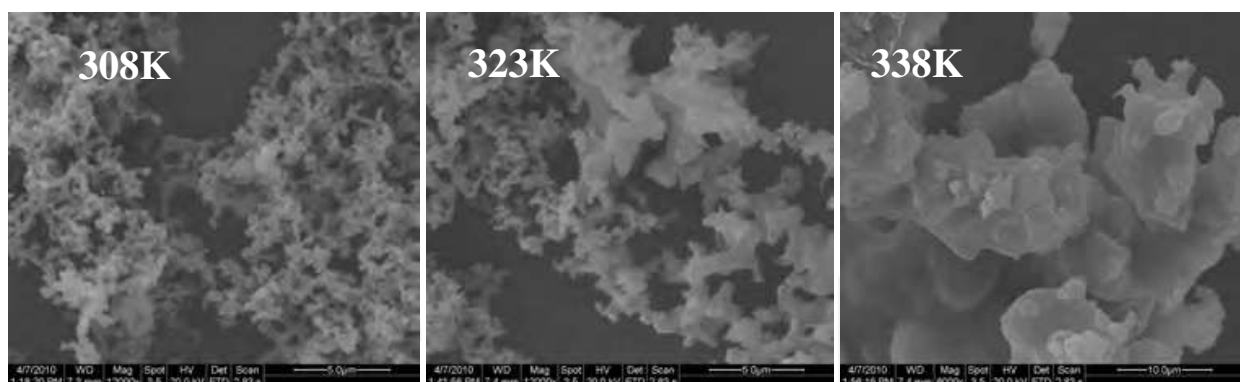

Fig. 3. SEM images of amoxicillin ethyl cellulose co-precipitated (Montes et al., 2011b).

because all the active substance could be situated on the surface of these microspheres and/or into the core. So, X-ray photoelectron spectroscopy (XPS) was used to determine the success of the encapsulation process by the chemical analysis of the particles on the precipitated surface (Morales et al., 2007). In this case, the elements that differentiate amoxicillin from ethyl cellulose are sulphur (S) and nitrogen (N) atoms. Therefore, these elements could indicate the location of the drug in the precipitated powders. On the other hand, amoxicillin delivery studies in simulated fluids from the co-precipitated obtained were carried out .The XPS spectra results were related to these drug delivery experiments and it was probed that the release of amoxicillin from precipitates in which N and S were

present on the surface is faster than in cases these elements were not. Anyway, all the co-precipitated materials allowed a slower drug release rate than pure drug.

On the other hand, in the RESS method, the sudden expansion of supercritical solution (solute dissolved in supercritical carbon dioxide) via nozzle and the rapid phase change at the exit of the nozzle cause a high super-saturation, thus causing very rapid nucleation of the substrate in the form of very small particles that are collected from the gas stream. Hence, the conditions inside the expansion chamber are a key factor to control particle size and the particles grow inside the expansion chamber to their final size. This result clarifies the influence of two important process parameters on particle size. Both, a shorter residence time and, hence, less time available for particle growth as well as a higher dilution of the particles in the expansion chamber result in smaller particles.

3.1 Parameters influence on hydrodynamic

Mass transfer is one of the key factors that control the particle size in the SAS process. This is influenced by both the spray hydrodynamics of the organic solution and the thermodynamic properties of the supercritical fluid phase.

In the last years, the hydrodynamic of the SAS process has been the subject of several papers. Most authors face up to this problem considering that the jet of organic solvent behaves like a liquid jet injected into a gas, allowing to apply the classic theory of jet break-up. This theory could be applied successfully at subcritical conditions, below the mixture critical point solvent-CO_2, where there is surface tension. The mixture critical point denotes the limit of the two-phase region of the phase diagram. In other words, this is the point at which an infinitesimal change in some thermodynamic variable such as temperature or pressure will lead to separation of the mixture into two distinct phases.

However, in supercritical conditions, above the critical point of the mixture organic solvent and CO_2, it is not possible to distinguish droplets nor interfaces between the liquid solution and the phase of dense CO_2 gas. Surface tension decreases to zero in a shorter distance than characteristic break-up lengths. Thus, the jet spreads forming a gaseous plume and will be characterized by the degree of turbulence associated with the vortices produced in the SC CO_2 (Chehroudi et al., 2002; Kerst et al., 2000; Reverchon et al., 2010). Lengsfeld et al. were the first group that investigated fluid dynamics of the SAS process, studying the evolution and disappearance of the liquid surface tension of fluids injected in supercritical carbon dioxide. They concluded that a gas-like jet is formed after the jet break-up (Lengsfeld et al., 2000). In this way, Kerst et al. determined the boundaries between the different modes and they noted a strong interdependence between mass transfer and fluid dynamics (Kerst et al., 2000).

In the SAS related literature there is a general agreement about the flow regimes observable when a liquid is injected in a vessel. The way in which the liquid solution is dispersed in the CO_2 when the operating conditions are below the mixture critical point (MCP), which is strongly influenced by the operating pressure and the flow rate of liquid solution at fixed temperature, can be described according to one of the following four regimes: 1) the dripping mode, which requires lower flow speed so that drops can detach themselves from the orifice, 2) the Rayleigh break up regime, which is characterized by a rupture of the jet in the form of monodisperse droplets, 3) the sine wave break up regime, in which a helicoidal oscillation of the jet occurs, leading to its rupture into droplets with a polydisperse distribution, and 4) atomization, in which the jet is smooth when it leaves the orifice, until it reaches the zone of highly chaotic rupture where a cone of atomized liquid is formed.

When SAS is performed at supercritical conditions a transition between multi-phase and single-phase mixing is observed by increasing the operating pressure. Single-phase mixing is due to the very fast disappearance of the interfacial tension between the liquid solvent and the fluid phase in the precipitator. The transition between these two phenomena depends on the operating pressure, but also on the viscosity and the surface tension of the solvent. Reverchon et al. demonstrates that in the case of dimethyl sulfoxide (DMSO) at pressures larger than the MCP a progressive transition exists between multi-phase and single-phase mixing, but is not observed, even for pressures very close to the MCP, in the case of acetone (Reverchon et al., 2010). In the dripping mode, the droplet size decrease with increase in pressure operation due to a corresponding decrease in the interface tension, so the initial droplet size can be manipulated by small changes in the pressure of CO_2 (Lee et al., 2008).

However, in the Rayleigh disintegration mode, the droplet size is weakly dependent on the interface tension of the system and is proportional to the diameter of the jet. In the dripping mode, the size and shape of the drops become highly dependent on the nozzle exit condition.

Sometimes, the transition between multi-phase (formation of droplets after jet break-up) and single-phase mixing (no formation of droplets after jet break-up) could not be located at the pressure of the mixture critical point. Dukhin et al. (Dukhin et al., 2003) and Gokhale et al. (Gokhale et al., 2007) found that jet break-up into droplets still takes place at pressures slightly above the MCP. Due to the non-equilibrium conditions during mixing, there is a dynamic (transient) interfacial tension that decreases between the inlet of the liquid and its transformation to a gas-like mixture. The transition between these multi-phase and single-phase mixing depends on the operating pressure, but also on the viscosity and the surface tension of the solvent.

Not only the thermodynamics but also the nozzle device or liquid solution flow rate will influence on the observed regime. The kind of injection device and its orifices diameter will determine the chosen liquid solution flow rate to get a successful jet break up. In this way, in a previous work, when the 200 µm diameter nozzle was used with a liquid flow rate of 1mL/min, the solution was not atomized, and we did not obtain any precipitation (Tenorio et al., 2009).

A lot of parameters control the precipitation process and many particle morphologies have been observed. As it was commented before, the kind of injection device used (and its efficiency), can strongly influence the precipitation process. The objective of these devices in SAS processing is to produce a very large contact surface between the liquid and the fluid phase, to favour the mass transfer between the antisolvent and the liquid solvent inducing jet break-up and atomization of the liquid phase.

Various injection devices to produce liquid jet break-up have been proposed in the literature. Yeo et al. (Yeo et al., 1993) proposed the adoption of a nozzle and tested various nozzle diameters ranging from 5 to 50 µm. Moussa et al. (Moussa et al., 2005) showed that the pressure distribution during the expansion of the supercritical fluid is a function of the nozzle length and diameter. Other authors used small internal diameter capillaries (Dixon et al., 1993; Randolph et al., 1993). Coaxial devices have also been proposed: in the SEDS process (solution enhanced dispersion by supercritical fluids) a coaxial twin-fluid nozzle to co-introduce the SCF antisolvent and solution is used (Bałdyga et al., 2010; He et al., 2010; Mawson et al., 1997; Wena et al., 2010). Complex nozzles geometries have also been tested carrying out a comparative study of the nozzle by computational fluid dynamics (Balabel et

al., 2011; Bouchard et al., 2008). Petit-Gas et al. found that for the lowest capillary internal diameter studied, there were particles with differences morphologies according to the jet velocity. For the lowest jet velocity, irregular morphology was obtained, and for highest jet velocity spherical morphology was obtained (Petit-Gas et al., 2009). However, for the highest capillary internal diameter experiments, particles morphology difference was less important. Particles were quasi-spherical, to a lesser extent for the smallest jet velocity. Once more time it was demonstrated the parameters interrelation in SAS process and its great complexity. Not only the kind of nozzle but also the nozzle relative position to CO_2 inlet must be taken into account. In this way, Martin & Cocero studied the differences on hydrodynamics and mixing when CO_2 is not introduced through the concentric annulus, but through a different nozzle, which is placed relatively far from the nozzle of the organic solution. Since the inlet velocity of CO_2 is much lower than the inlet velocity of the solution, this flow has a relatively small influence on hydrodynamics and mixing. However, if CO_2 is not introduced through the annulus, the fluid that diffuses into the jet is no longer almost pure CO_2, but fluid from the bulk fluid phase, which has some amount of organic solvent. This greatly reduces the supersaturation and bigger particles are formed (Martin & Cocero, 2004).

Moreover, these different unstable modes (Rayleigh break up, sine wave break up and atomization) are controlled by several competing effects: capillary, inertial, viscous, gravity and aerodynamic effects (Petit-Gas et al., 2009). The predominance of each effect has been discussed in several works (Badens et al., 2005; Carretier et al., 2003; Kerst et al., 2000). Reynolds number gives a measure of the ratio of inertial forces to viscous forces. For the lower Reynolds numbers, Rayleigh regime is observed and surface tension is the chief force controlling the break-up of an axisymmetrical jet. For higher Reynolds numbers, the inertial forces compete with the capillary forces. There is a lateral motion in the jet break-up zone which leads to the formation of an asymmetrical jet, which can be either sinuous or helicoidal. Finally, when the flow rate goes beyond a certain value, the aerodynamic effects become quite strong and the jet is atomised. Another dimensionless number frequently used to describe jet fluid dynamics is the Ohnesorge (Oh) number that relates the viscous and the surface tension force by dividing the square root of Weber number by Reynolds number (Badens et al., 2005; Czerwonatis, 2001; Kerst et al., 2000).

In this way, taking into account the critical atomization velocity defined as the velocity corresponding to the boundary between the asymmetrical mode and the atomization mode, it is possible to tune the process towards one or another regime. Moreover this critical velocity seems to be dependent on CO_2 density. Badens et al. observed a decrease in this critical jet velocity when the CO_2 continuous phase density increases (Badens et al., 2005). Badens et al. and Czerwonatis et al. found out the predominant effect of the continuous phase properties on jet break-up, especially in the asymmetrical and direct atomization modes because of the aerodynamic forces preponderance (Badens et al., 2005; Czerwonatis et al., 2001). However Petit-Gas et al. concluded that variations of the continuous phase properties had no effects on the transition velocity in the studied conditions (Petit-Gas et al., 2009).

3.2 Morphology

Some authors attempted to connect the observed flow or mixing regimes to the morphology of the precipitated particles. Lee et al. injected a solution of dichloromethane (DCM) and poly lactic acid (PLA) at subcritical conditions in the dripping and in the Rayleigh

disintegration regimes and observed the formation of uniform PLA microparticles (Lee et al., 2008). Other authors (Chang et al., 2008; Gokhale et al., 2007; Obrzut et al., 2007; Reverchon et al., 2008) did not find relevant differences in the various precipitates obtained. Particularly, PLA morphologies showed to be insensitive to the SAS processing conditions (Randolph et al., 1993). This characteristic fact could be assigned to the high molecular weights and the tendency to form aggregated particles because of the reduction of the glass transition temperature in SC-CO$_2$.

At subcritical conditions the interfacial tension between the injected liquid and the bulk phase never goes to zero and a supercritical mixture is not formed between the liquid solvent and CO$_2$. The droplets formed during atomization are subjected to a very fast internal formation of a liquid/CO$_2$ mixture. Due to a high solubility of CO$_2$ in pressurized organic liquids and a very poor evaporation of organic solvents into the bulk CO$_2$, the droplets expand. During these processes, the interfacial tension allows the droplets to maintain its spherical shape, even when the solute is precipitated within the droplet. Saturation occurs at the droplet surface and solidification takes place with all solutes progressively condensing on the particle internal surface. The final result is the formation of a solid shell.

This kind of particles has also been observed in other SAS works (Reverchon et al., 2008). It has been also obtained expanded hollow particle at same conditions. The different surface morphologies can depend on different controlling mass transfer mechanisms, as suggested by Duhkin et al. (Duhkin et al., 2005).

Operating conditions above the MCP, from a thermodynamic point of view, are characterized by zero interfacial tension. But, the liquid injected into the precipitator, before equilibrium conditions are obtained, experiences the transition from a pure liquid to a supercritical mixture. Therefore, interfacial tension starts from the value typical of the pure liquid and progressively reduces to zero. This fact means that droplets formed after jet break-up (whose presence indicates in every case the existence of an interfacial tension) are formed before the disappearance of the interfacial tension. In other words, the time of equilibration is longer than the time of jet break-up and spherical microparticles instead of nanoparticles can be obtained.

3.3 Visualization techniques

Many researchers have used imaging and visualization techniques to study jet flows, atomization, and droplets; a number of systems are reviewed in the literature (Bell et al., 2005; Chigier et al.,1991). Jet lengths and spray widths ranging to milimeters and drop and particle sizes ranging to micrometers must be taking into account in order to select imaging system components.

Several studies used particle and droplet visualization in supercritical fluids (Badens et al., 2005; Gokhale et al.,2007; Kerst et al.,2000; Lee et al.,2008; Mayer & Tamura,1996; Obrzut et al.,2007; Randolph, et al., 1993; Shekunov et al., 2001).

The optical technique described in these works provides the ability to visualize mixing occurring between two fluids with different refractive indices. For instance, shadowgraphy is an optical method to obtain information on non-uniformities in transparent media, independently if they arise by temperature, density or concentration gradients. All of these inhomogeneities refract light which causes shadows.

Although for SAS precipitation, microscopy-base imaging offers the advantage of examining the dynamic process that leads to particle formation, the presence of particles smaller than two microns complicates an already difficult task of imaging an injection process.

The ability to identify and characterize these small formations drives future system improvements, including lighting enhancements laser-induced fluorescence, and higher spatial resolution cameras. In this way Reverchon et al. used light scattering technique to clearly differentiate between an atomized very droplet laden spray and a dense "gas-plume", limitation which cannot be gained by applying optical techniques due to the fact that both the droplet laden spray and the dense "gas-plume" result in a dark shadow (Reverchon et al., 2010).

On the other hand, extensive research has been done using scanning electron microscopy (SEM) to evaluate the size and morphology of particles formed under supercritical conditions (Armellini& Tester, 1994; Bleich et al., 1994; Mawson et al. 1997; Randolph et al., 1993; Shekunov et al., 2001;). A limitation of SEM analysis is that it is applied to particles after they have been removed from the dynamic system.

4. A particular case: Ampicillin SAS precipitation

In our research group a study was carried out to establish a correlation between the morphologies of the particles obtained in the ampicillin precipitation assays and the estimated regimes. This correlation would be an ideal tool to establish the limiting hydrodynamic conditions for the success of the test in order to define the successful experiments; that is, the appropriate conditions to orientate the process toward the formation of uniform spherical nanoparticles instead of irregular and larger-sized particles, for the solute-solvent-SC CO_2 system studied (Tenorio et al.,2009).

A series of ampicillin precipitation experiments by the SAS technique, utilizing N-methyl-pyrrolidone (NMP) as the solvent and CO_2 as the antisolvent, under different operating conditions were carried out. Two nebulizers, with orifice diameters of 100 and 200 μm, respectively were used.

A pilot plant, developed by Thar Technologies® (model SAS 200) was used to carry out all the experiments. A schematic diagram of this plant is shown in Figure 4. The SAS 200 system comprises the following components: two high-pressure pumps, one for the CO_2 (P1) and the other for the solution (P2), which incorporate a low-dead-volume head and check valves to provide efficient pumping of CO_2 and many solvents; a stainless steel precipitator vessel (V1) with a 2L volume consisting of two parts, the main body and the frit, all surrounded by an electrical heating jacket (V1-HJ1); an automated back-pressure regulator (ABPR1) of high precision, attached to a motor controller with a position indicator; and a jacketed (CS1-HJ1) stainless steel cyclone separator (CS1) with 0.5L volume, to separate the solvent and CO_2 once the pressure was released by the manual back-pressure regulator (MBPR1).The following auxiliary elements were also necessary: a low pressure heat exchanger (HE1), cooling lines, and a cooling bath (CWB1) to keep the CO_2 inlet pump cold and to chill the pump heads; an electric high-pressure heat exchanger (HE2) to preheat the CO_2 in the precipitator vessel to the required temperature quickly; safety devices (rupture discs and safety valve MV2); pressure gauges for measuring the pump outlet pressure (P1, PG1), the precipitator vessel pressure (V1, PG1), and the cyclone separator pressure (CS1, PG1); thermocouples placed inside (V1-TS2) and outside (V1-TS1) the precipitator vessel, inside the cyclone separator (CS1-TS1), and on the electric high pressure heat exchanger to obtain continuous temperature measurements; and a FlexCOR Coriolis mass flowmeter (FM1) to measure the CO_2 mass flow rate and another parameters such as total mass, density, temperature, volumetric flow rate, and total volume.
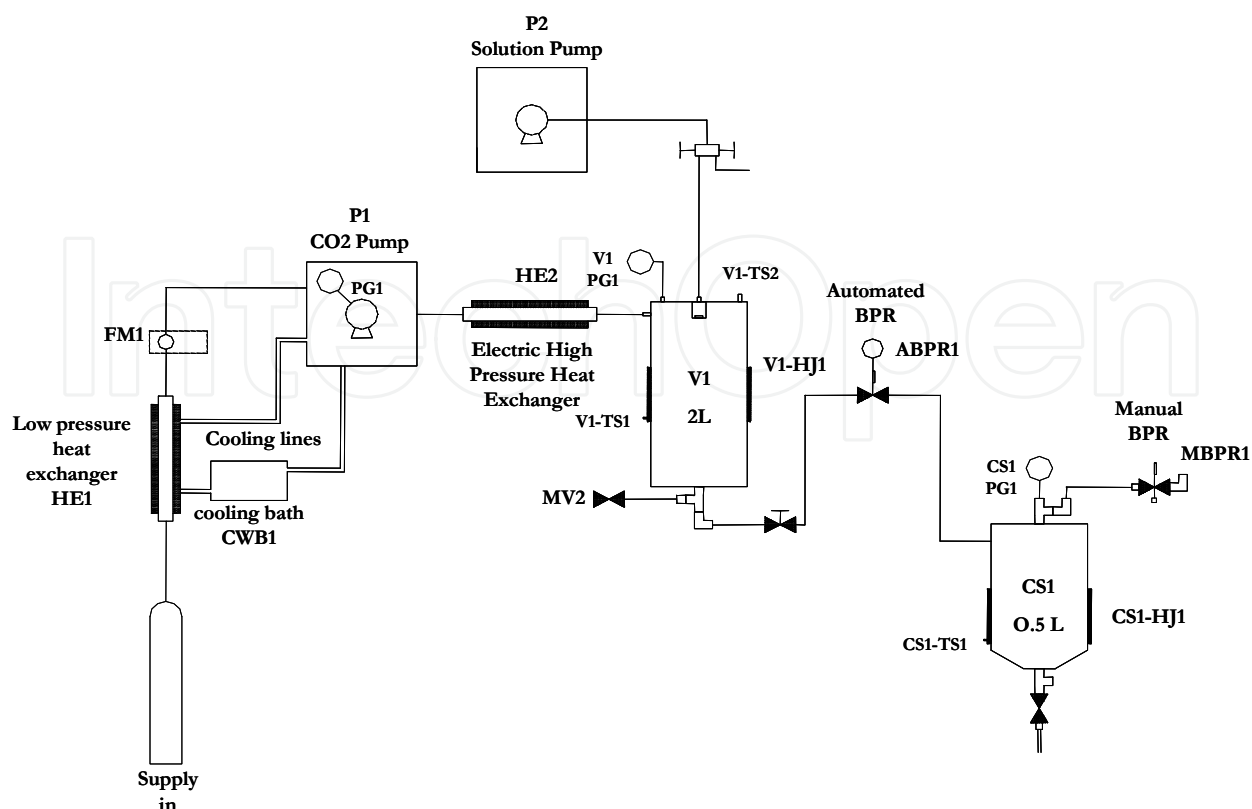
Fig. 4. Schematic diagram of the pilot plant

The pendant droplet method, as introduced by Andreas and Tucker, was used to determine the interfacial tension between NMP and SC CO_2 (Andreas&Tucker, 1938).This method, and its application to high pressures and temperatures, are comprehensively described by Jaeger (Jaeger et al., 1996). A commercial CCD video technique allows recording of droplet shapes for subsequent video image processing.

Rayleigh breakup, sinusoidal wave break up, and atomization regimes are seen to be clearly differentiated by representing graphically the Reynolds number against Ohnesorge number Here, the forces of inertia of the liquid phase (pressure gradient), the forces of capillarity (surface tension), and those of viscosity of the liquid phase (friction) are taken into account, but the force of gravity is considered to be negligible.

Two differentiated types of morphology can be identified in the precipitated experiments: spherical nanoparticles of ampicillin that are obtained from a fine precipitate with foamy texture, and particles of ampicillin with irregular forms and larger size, which are characteristic of the precipitate formed by aggregates, compact films, and rods (Figure 5).

The aim of the work is to explain, from the estimation of the different disintegration regimes as a function of the physicochemical properties and of the velocity of the jet, the two different morphologies obtained in the ampicillin precipitation experiments for a specific range of operating conditions. Thus it should be possible to specify the hydrodynamic conditions for orientating the process toward the formation of uniform spherical nanoparticles rather than larger size irregular particles.

The morphology of the precipitate obtained at low pressure was supposed to be in accordance with the Rayleigh estimated regime, since droplets with a diameter of approximately twice the diameter of the orifice would be produced; (Badens et al., 2005)
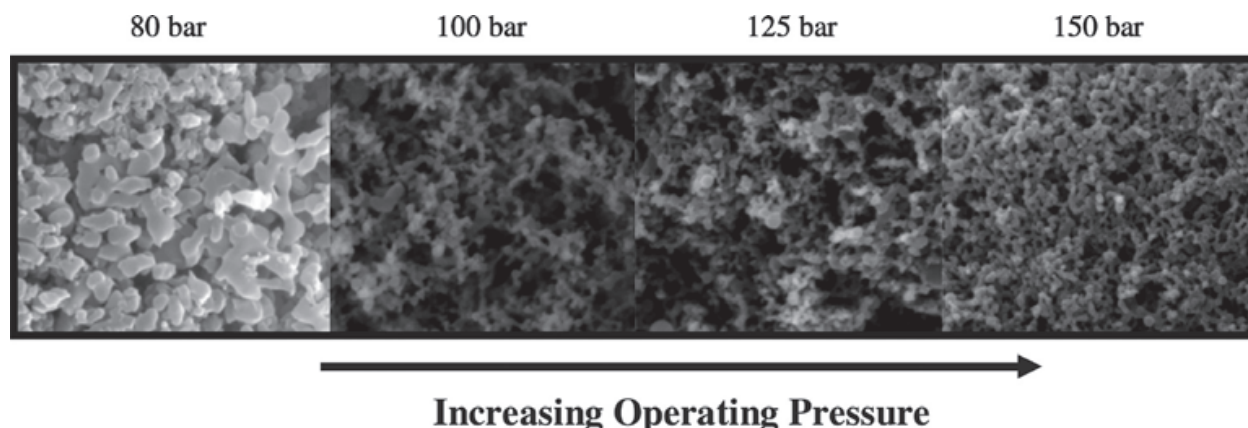
Increasing Operating Pressure

Fig. 5. Effect of operating pressure on microstructure of ampicillin powder obtained by the SAS experiments (Tenorio et al., 2009).

then, because sufficient contact area would not be generated, the liquid phase does not evaporate in the dense phase of the CO_2. Instead, the liquid droplets accumulate in the filter, where the precipitate is obtained by the drying action of the CO_2.

In contrast, for higher pressures, the presence of a precipitate occurring as aggregates in the filter may be explained by the existence of significant mechanisms that stabilize the liquid jet. These important mechanisms of stabilization may be associated with the existence of the dynamic interfacial tension (Dukhin et al., 2003).Therefore, the so-called "gaseous plume" or "gas-like jet", which is characteristic of states of complete miscibility of mixtures (above their MCP),would not be produced, even at 150 bar.

The influence of the mean velocity of the jet of liquid solution was also analyzed. The liquid solution flow rate from 1 mL/min to 5 mL/min causes the jet to disintegrate, passing through the three possible regimes: Rayleigh, sine wave break-up and atomization. The lowest flow rate tested (1 mL/min), which is equivalent to a jet velocity of 0.5 m/s (200 µm nozzle diameter), led to an unsatisfactory test result, which may be in agreement with the Rayleigh-type estimated regime; this is because the droplets that formed would not generate sufficient contact area to produce saturation while they are in motion, and, consequently, ampicillin is not precipitated. When the liquid solution flow rate is increased to 2 mL/min a dispersion of the sine wave breakup type is estimated. Considering that a polydisperse
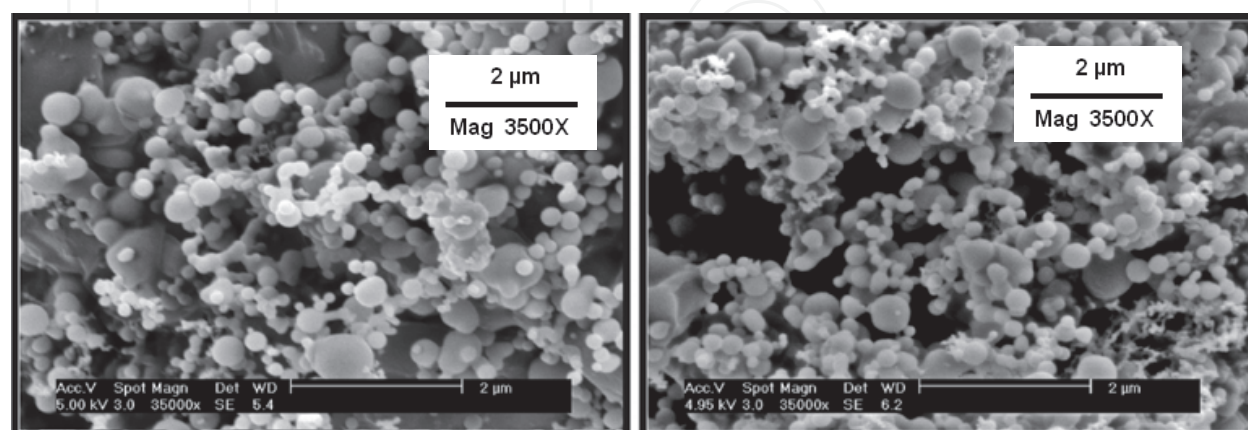

Fig. 6. SEM images showing the microstructure of the ampicillin powder obtained by SAS experiment with 5ml/min (at 180 bar, 328 K, and 200 µm) (Tenorio et al., 2009).

distribution of droplets is produced in this regime, it is very well correlated with the experimental obtained results (Tenorio et al., 2009).

When the flow rate is increased to 3 mL/min, it is estimated that the transition is complete, and the liquid is atomized. The large quantity of fine precipitate with foamy texture obtained both on the walls and accumulated in the filter (characteristic of nanoparticles) would have originated from the fully atomized and homogeneous dispersion that is occurring in the precipitation chamber. With 5 mL/min it was obtained similar results in accordance with the estimated atomization regime (Figure 6).

5. Conclusions

The hydrodynamics of the SAS process has been revised. Nozzle device, liquid flow rate and pressure effects on hydrodynamics have been taken into account. Flow regimes observable in the SAS related literature have been described. Dripping mode is simply due to the use of liquid flow rates that are too low to produce a continuous liquid flow and do not produce atomization. Rayleigh breakup, sinusoidal wave break up, and atomization regimes and, particularly their competition at some process conditions require a detailed analysis. The ability to identify and characterize these regimes drives future system improvements, including lighting enhancements laser-induced fluorescence, and higher spatial resolution cameras.

Morphology of the precipitated particles can be related to flow or mixing regimes. In the ampicillin case, two differentiated types of morphology can be identified in the precipitated experiments: spherical nanoparticles of ampicillin that are obtained from a fine precipitate with foamy texture, and particles of ampicillin with irregular forms and larger size, which are characteristic of the precipitate formed by aggregates, compact films, and rods. It has been correlated the morphologies of the particles obtained in the ampicillin precipitation assays and the estimated regimes as a function of the physicochemical properties and of the velocity of the jet, for a specific range of operating conditions.

However, the results from the application of these correlations cannot explain the morphologies of the precipitates obtained in some experiments. This fact can be due to important stabilization mechanisms as dynamic interfacial tension

Due to the great complexity of the SAS process, factors such as the ternary phase equilibrium, matter transfer between the phases, and the kinetics of nucleation and growth need to be considered, in addition to the limiting hydrodynamic conditions.

6. Acknowledgment

7. References

Andreas, J. M.; Tucker, W. B. (1938). Boundary Tension by Pendant Drop.*J. Phys. Chem.*,42, pp. 1001-1019.

Armellini, F.J., Tester, J.W. (1994). Precipitation of sodium chloride and sodium sulfate in water from sub- to supercritical conditions:150 to 550ºC, 100 to 300 bar. *J. Supercrit. Fluids*, 7, pp.147–158.

Badens, E., Boutin, O., Charbit, G. (2005). Laminar jet dispersion and jet atomization in pressurized carbon dioxide, *J. Supercrit. Fluids* ,36, pp. 81–90.

Balabel, A., Hegab, A.M., Nasr, M., El-Behery, S. M. (2011). Assessment of turbulence modeling for gas flow in two-dimensional convergent–divergent rocket nozzle. *Appl. Math. Model.*, 35, pp. 3408–3422.

Bałdyga, J., Kubicki, D., Shekunov, B.Y., Smithd, K.B. (2010). Mixing effects on particle formation in supercritical fluids, *Chem. Eng. Res. Des.*, 88, pp. 1131–1141.

Bell, P. W., Stephens, A. P.,Roberts, C. B., Duke, S. R. (2005). High-resolution imaging of the supercritical antisolvent process, *Experiments in Fluids*, 38, pp. 708–719.

Benedetti, L., Bertucco, A., Pallado, P. (1997). Production of micronic particles of biocompatible polymer using supercritical carbon dioxide, *Biotechnol. Bioeng.*, 53, pp. 232-237.

Bleich, J., Cleinebudde, P., Muller, B.W. (1994). Influence of gas density and pressure on microparticles produced with the ASES process, *Int. J. Pharm.*, 106, pp. 77–84.

Bouchard, A., Jovanovic, N., A. H. de Boer, Martín, A., Jiskoot, W., Crommelin, D. J.A. , Hofland, G.W., Witkamp, G.-J. (2008). Effect of the spraying conditions and nozzle design on the shape and size distribution of particles obtained with supercritical fluid drying, *Eur. J. Pharm. Biopharm.*, 70, pp. 389–401.

Carretier, E., Badens, E., Guichardon, P., Boutin, O., Charbit, G. (2003). Hydrodynamics of supercritical antisolvent precipitation: characterization and influence on particle morphology, *Ind. Eng. Chem. Res.*, 42, pp. 331–338.

Czerwonatis, N., Eggers, R., Charbit, G. (2001). Disintegration of liquid jets and drop drag coefficients in pressurized nitrogen and carbon dioxide, *Chem. Eng. Tech.*, 24, pp. 619–624.

Chang, S.-C., Lee, M.-J., Lin, H.-M. (2008). Role of phase behavior in micronization of lysozyme via a supercritical anti-solvent process, *Chem. Eng. J.*, 139, pp. 416–425.

Chehroudi, B., Cohn, R., Talley, D. (2002). Cryogenic shear layers: experiments and phenomenological modelling of the initial growth rate under subcritical and supercritical conditions, *Int. J. Heat Fluid Flow*, 23, pp. 554-563.

Chigier, N. (1991). Optical imaging of sprays. *Prog. Energy Combust. Sci.*, 17, pp.211–262

Dixon, D.J., Johnston, K.P., Bodmeier, R.A. (1993).Polymeric materials formed by precipitation with a compressed fluid antisolvent, AIChE J., 39 (1), pp. 127–139.

Dukhin, S.S., Zhu, C., Pfeffer, R., Luo, J.J., Chavez, F., Shen, Y. (2003). Dynamic interfacial tension near critical point of a solvent–antisolvent mixture and laminar jet stabilization, *Physicochem. Eng. Aspects*, 229, pp. 181-199.

Dukhin, S. S., Shen, Y., Dave, R., Pfeffer, R. (2005). Droplet mass transfer, intradroplet nucleation and submicron particle production in two-phase flow of solvent-supercritical antisolvent emulsion. *Colloids Surf. A*, 261, pp. 163-176.

Elvassore, N., Bertucco, A., Caliceti, P. (2001). Production of insulin-loaded poly(ethylene glycol)/poly(l-lactide) (PEG/PLA) nanoparticles by gas antisolvent techniques, *J. Pharm. Sci.*, 90, pp. 1628-1636.

Falk, R.F., Randolph, T.W. (1998). Process variable implications for residual solvent removal and polymer morphology in the formation of gentamycin-loaded poly (L-lactide) microparticles, *Pharm. Res.*, 15, pp. 1233-1237.

Giunchedi, P., Genta, I., Conti, B., Conte, U., Muzzarelli, R.A.A. (1998) .Preparation and characterization of ampicillin loaded methylpyrrolidinone chitosan and chitosan microspheres, *Biomat.*, 19, pp.157-161.

Gokhale, A., Khusid, B., Dave, R.N., Pfeffer, R. (2007).Effect of solvent strength and operating pressure on the formation of submicrometer polymer particles in supercritical microjets, *J. Supercrit. Fluids* ,43, pp 341-356.

He, W., Jiang, Z., Suo, Q.,Li, G. (2010). Mechanism of dispersing an active component into a polymeric carrier by the SEDS-PA process, *J. Mater. Sci.*, 45, pp. 467–474.

Jaeger, Ph T.; Schnitzler, J. V.; Eggers, R. (1996). Interfacial Tension of Fluid Systems Considering the Non-Stationary Case with Respect to Mass Transfer. *Chem. Eng. Technol.*, 19, pp.197.

Jung, J., Perrut., M. (2001). Particle design using supercritical fluids: Literature and patentsurvey. *J. Supercrit. Fluids*, 20 (3), pp. 179-219.

Kerst, A.W., Judat, B., Schlünder, E.U. (2000).Flow regimes of free jets and falling films at high ambient pressure, *Chem. Eng. Sci.*, 55, pp. 4189-4208.

Lee, L.Y., Lim L. K., Hua, J., Wang, C.-H. (2008). Jet breakup and droplet formation in near-critical regime of carbon dioxide-dichloromethane system, *Chem.Eng. Sci.*, 63, pp. 3366-3378.

Lengsfeld, C.S., Delplanque, J.P., Barocas, V.H., Randolph, T.W. (2000).Mechanism governing microparticle morphology during precipitation by a compressed antisolvent: atomization vs nucleation and growth, *J. Phys. Chem. B*, 104, pp. 2725–2735.

Lora, M., Bertucco, A., Kikic, I. (2000). Simulation of the Semicontinuous Supercritical Antisolvent Recrystallization Process. *Ind. Eng. Chem. Res.*, 39, pp. 1487-1496.

Martín, A., Cocero, M.J. (2004). Numerical modeling of jet hydrodynamics, mass transfer, and crystallization kinetics in the supercritical antisolvent (SAS) process *J. Supercrit. Fluids*, 32, pp. 203–219.

Martín, A., Cocero, M.J. (2008).Precipitation processes with supercritical fluids: patents review, *Recent Patents Eng.* 2, pp.9 -20.

Mawson S, Kanakia S, Johnston KP. (1997). Coaxial nozzle for control of particle morphology in precipitation with a compressed fluid antisolvent, *J. Appl. Polym. Sci.*, 64:, pp. 2105-2118.

Mayer, W.,Tamura, H. (1996). Propellant injection in a liquid oxygen/ gaseous hydrogen rocket engine. *J. Propul. Power*, 12(6), pp.1137–1147.

Moneghini, M., Kikic I., Voinovich, D., Perissutti, B., Filipovic-Grcic, J. (2001). Processing of carbamazepine - PEG 4000 solid dispersions with supercritical carbon dioxide: Preparation, characterisation, and in vitro dissolution, *Int. J. Pharm.*, 222, pp.129-138.

Montes, A., Tenorio, A., Gordillo, M.D., Pereyra, C., Martínez de la Ossa, E. (2010). Screening design of experiment applied to supercritical antisolvent precipitation of amoxicillin: exploring new miscible conditions. *J. Supercrit. Fluids*, 51, pp. 399-403.

Montes, A., Tenorio, A., Gordillo, M.D., Pereyra, C., Martínez de la Ossa, E. (2011a). Supercritical Antisolvent Precipitation of Ampicillin in Complete Miscibility Conditions. *Ind. Eng. Chem. Res.*, 50, pp. 2343–2347.

Montes, A., Gordillo, M.D., Pereyra, C., Martínez de la Ossa, E. (2011b). Co-precipitation of amoxicillin and ethylcellulose microparticles by supercritical antisolvent process *J. Supercrit. Fluids* (in press).

Morales, M. E., Ruiz, M. A., Oliva, I., Oliva, M., Gallardo, V. (2007). Chemical characterization with XPS of the surface of polymer microparticles loaded with morphine. *Int. J. Pharm.*, 333, pp. 162-166.

Moussa, A. B., Ksibi, H., Tenaud, C., Baccar, M. (2005). Parametric study on the nozzle geometry to control the supercritical fluid expansion, *Int. J. Thermal Sciences*, 44, pp. 774–786.

Obrzut, D.L., Bell, P.W., Roberts, C.B., Duke, S.R. (2007). Effect of process conditions on the spray characteristics of a PLA plus methylene chloride solution in the supercritical antisolvent precipitation process, *J. Supercrit. Fluids*, 42, pp. 299–309.

Okada, H., Toguchi, H. (1995). Biodegradable microspheres in drug delivery, *Crit. Rev. in Ther. Drug Carrier Syst.*, 12, pp. 1-99.

Ozcan, A.S.; Clifford, A.A.; Bartle, K.D. and Lewis, D.M. (1998). Dyeing of cotton fibres with disperse dyes in supercritical carbon dioxide, *Dyes and Pigments*, 36(2), pp. 103-110.

Petit-Gas, T., Boutin, O., Raspo, I., Badens, E. (2009). Role of hydrodynamics in supercritical antisolvent processes, *J. Supercrit. Fluids* , 51, pp. 248–255.

Randolph, T.W., Randolph, A.D., Mebes, M., Yeung, S. (1993). Sub-micrometer-sized biodegradable particles of poly(L- lactic acid) via the gas antisolvent spray precipitation process, *Biotechnol. Progress*, 9, pp. 429-435.

Reverchon, E., Della Porta, G. (1999). Production of antibiotic micro- and nano-particles by supercritical antisolvent precipitation, *Powder Technol.*, 106, pp. 23-29.

Reverchon, E. (2002). Supercritical-assisted atomization to produce micro- and/or nanoparticles of controlled size and distribution, *Ind. Eng. Chem. Res.*, 41, pp. 2405-2411.

Reverchon, E., Adami, R., Caputo, G., De Marco, I. (2008).Expanded microparticles by supercritical antisolvent precipitation: interpretation of results. *J. Supercrit.Fluids*, 44(1), pp. 98–108.

Reverchon, E.; Torino, E.; Dowy, S.; Braeuer, A.; Leipertz, A. (2010). Interactions of phase equilibria, jet dynamics and mass transfer during supercritical antisolvent micronization. *Chem. Eng. J.,* 156, pp. 446-458.

Reverchon, E., De Marco, I. (2011). Mechanisms controlling supercritical antisolvent precipitate morphology. *Chem. Eng. J.* (In press).

Shariati, A., Peters. C. J. (2003). Recent developments in particle design using supercritical fluids, *Curr. Opin. Solid State Mater. Sci.*, 7, (4–5) pp. 371-383.

Shekunov, B. Yu., Baldyga, J., York, P. (2001). Particle formation by mixing with supercritical antisolvent at high Reynolds numbers. *Chem. Eng. Sci.*, 56, pp. 2421-2433.

Subramaniam, B., Snavely, K., Rajewski, R.A. (1997). Pharmaceutical processing with supercritical carbon dioxide, J. Pharm. Sci., 86, pp. 885-890.

Tenorio, A., Gordillo, M. D., Pereyra, C.M., Martínez de la Ossa, E.J. (2007a). Controlled submicro particle formation of ampicillin by supercritical antisolvent precipitation, *J. Supercrit. Fluids*, 40, pp. 308-316.

Tenorio, A.; Gordillo, M. D.; Pereyra, C. M.; Martínez de la Ossa, E. M. (2007b). Relative importance of the operating conditions involved in the formation of nanoparticles of ampicillin by supercritical antisolvent precipitation. *Ind. Eng. Chem. Res.*, 46, pp. 114-123.

Tenorio, A., Gordillo, M. D., Pereyra, C.M., Martínez de la Ossa, E.J. (2008). Screening design of experiment applied to supercritical antisolvent precipitation of amoxicillin, *J. Supercrit. Fluids*, 44, pp. 230-237.

Tenorio, A., Jaeger, P., Gordillo, M.D., Pereyra, C.M., Martínez de la Ossa, E.J. (2009). On the selection of limiting hydrodynamic conditions for the SAS process, *Ind. Eng. Chem. Res.,*48 (20), pp. 9224–9232.

Wena, Z., Liua, B., Zhenga, Z., Youa, X., Pua, Y., Li, Q. (2010). Preparation of liposomes entrapping essential oil from Atractylodes macrocephala Koidz by modified RESS technique, *Chem. Eng. Res. Des.*, 88, pp. 1102–1107.

Winters, M.A., Knutson, B.L., Debenedetti, P.G., Sparks, H.G., Przybycien, T.M., Stevenson, C.L., Prestrelski, S.J. (1996). Precipitation of proteins in supercritical carbon dioxide, *J. Pharm. Sci.*, 85, pp. 586-594.

Yeo, S.-D., Lim, G.-B., Debenedetti, P.G., Bernstein, H. (1993). Formation of microparticulate protein powders using a supercritical fluid antisolvent, *Biotechnol. Bioeng.*, 41, pp. 341-346.
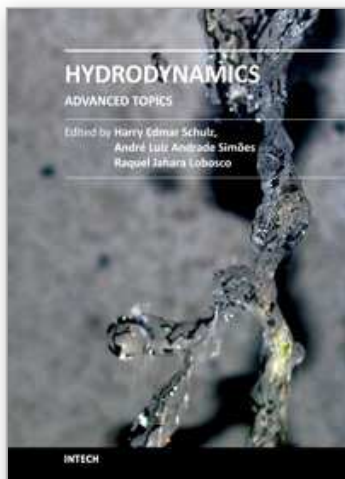
Hydrodynamics - Advanced Topics

Edited by Prof. Harry Schulz

The phenomena related to the flow of fluids are generally complex, and difficult to quantify. New approaches - considering points of view still not explored - may introduce useful tools in the study of Hydrodynamics and the related transport phenomena. The details of the flows and the properties of the fluids must be considered on a very small scale perspective. Consequently, new concepts and tools are generated to better describe the fluids and their properties. This volume presents conclusions about advanced topics of calculated and observed flows. It contains eighteen chapters, organized in five sections: 1) Mathematical Models in Fluid Mechanics, 2) Biological Applications and Biohydrodynamics, 3) Detailed Experimental Analyses of Fluids and Flows, 4) Radiation-, Electro-, Magnetohydrodynamics, and Magnetorheology, 5) Special Topics on Simulations and Experimental Data. These chapters present new points of view about methods and tools used in Hydrodynamics.

How to reference

In order to correctly reference this scholarly work, feel free to copy and paste the following:

A. Montes, A. Tenorio, M. D. Gordillo, C. Pereyra and E. J. Martinez de la Ossa (2011). Hydrodynamics Influence on Particles Formation Using SAS Process, Hydrodynamics - Advanced Topics, Prof. Harry Schulz (Ed.), ISBN: 978-953-307-596-9, InTech, Available from: http://www.intechopen.com/books/hydrodynamics-advanced-topics/hydrodynamics-influence-on-particles-formation-using-sas-process

INTECH
open science | open minds